Holocene and deglacial ocean temperature variability in the Benguela upwelling region: Implications for low-latitude atmospheric circulation

E. Christa Farmer[1] and Peter B. deMenocal

Department of Earth and Environmental Sciences and Lamont-Doherty Earth Observatory of Columbia University, Palisades, New York, USA

Thomas M. Marchitto

Department of Geological Sciences and Institute of Arctic and Alpine Research, University of Colorado, Boulder, Colorado, USA

Received 8 May 2004; revised 1 December 2004; accepted 28 February 2005; published 29 June 2005.

[1] Mg/Ca analyses of *G. bulloides* and abundances of *N. pachyderma* (left coiling) from Ocean Drilling Program (ODP) Leg 175 Hole 1084B in the Benguela coastal upwelling system document lower sea surface temperatures during the Last Glacial Maximum (LGM), Younger Dryas, mid-Holocene, and Little Ice Age in the southeastern Atlantic. Taking into consideration the possible effects of differential carbonate dissolution, the Mg/Ca data indicate Younger Dryas temperatures 2°–3°C cooler than those of the early Holocene and LGM temperatures 4°–5°C cooler than those of the early Holocene. The cool interval during the deglacial period at Hole 1084B matches the timing of Younger Dryas shifts in Cariaco Basin and Greenland Ice Sheet records and that of a nearby alkenone record. Comparison of mid-Holocene cooling at Hole ODP1084B with other high-resolution records of Holocene and last deglacial sea surface temperatures from the tropical Atlantic implies consistent basin-wide changes in atmospheric circulation. A brief period of 1.5°–2°C cooling between 17.8 and 17.2 ka, if related to Heinrich event 1, is consistent with a previously hypothesized tropical origin of all Heinrich climate change events.

Citation: Farmer, E. C., P. B. deMenocal, and T. M. Marchitto (2005), Holocene and deglacial ocean temperature variability in the Benguela upwelling region: Implications for low-latitude atmospheric circulation, *Paleoceanography*, *20*, PA2018, doi:10.1029/2004PA001049.

1. Introduction

[2] Millennial-scale climate changes during the last glacial cycle have been documented worldwide, but the underlying causes are still poorly understood. *Broecker* [2003] has reviewed the current state of understanding of Heinrich events, Dansgaard-Oeschger events, and the Younger Dryas, outlining the proposed mechanisms and highlighting existing data. One view is that teleconnections from the earth's tropics, stimulated by earth's orbital variations, drive at least some of these climate changes in distant, extratropical regions of the globe. The other main mechanism proposed for millennial-scale climate change involves reorganization of thermohaline deep ocean circulation, possibly forced by large inputs of freshwater to the North Atlantic from melting ice sheets.

[3] In the Zebiak-Cane coupled ocean-atmosphere model, certain precessional configurations were found to force El Niño–Southern Oscillation dynamics to lock into extreme states for centuries at a time [*Clement et al.*, 2001]. Eastern equatorial Pacific sea surface temperatures (SSTs) reconstructed from Mg/Ca of planktonic foraminifera appear to follow a precessional tempo [*Koutavas et al.*, 2002], as predicted by *Clement et al.* [2001]. In the tropical Atlantic, a proxy for thermocline depth also suggests that at least some millennial-scale events have a tropical origin [*McIntyre and Molfino*, 1996]. The authors suggest that the North African monsoon strengthened at two points in each precessional cycle over the last 45,000 years, during times when perihelion coincided with the summer solstice. This strengthening of the monsoon circulation would increase the meridionality of the southeastern trade winds and reduce equatorial upwelling, resulting in a deeper thermocline in the eastern tropical Atlantic. According to their hypothesis, this allowed warmer waters to enter the Gulf Stream and reach the North Atlantic, triggering ice sheet destabilization and the increased ice rafting associated with Heinrich events.

[4] The *McIntyre and Molfino* [1996] data indicate a deeper equatorial Atlantic thermocline during all known Heinrich events of the last 45,000 years. The periodicity of the thermocline signal in their record implies that a shift at 7.6 ka is also associated with the mechanism causing Heinrich events. They propose that the lack of high-latitude

[1] Now at Geology Department, Hofstra University, Hempstead, New York, USA.

0883-8305/05/2004PA001049$12.00

evidence for a Heinrich event in this time interval is consistent with their hypothesis that the primary forcing leading to Heinrich events originated in the tropics. This suggestion that Heinrich events were triggered from the tropics has been criticized for an imprecise explanation of why the North African monsoon should strengthen twice in each precessional cycle rather than once [*Berger and Loutre*, 1997], and for imprecise agreement between the timing of the changes in thermocline depth and the periodicities expected from theoretical calculations [*Kim et al.*, 2003]. More data are needed to corroborate these changes in tropical Atlantic Ocean and atmospheric circulation, and to confirm their timing, in order to strengthen conclusions about the source of climate variability during Heinrich events.

[5] Evidence for reorganization of thermohaline deep ocean circulation includes proxies for deep ocean nutrient concentrations, which show that North Atlantic Deep Water (NADW) formation decreased during the Younger Dryas [*Boyle and Keigwin*, 1987]. Increases in atmospheric radiocarbon inventories during the Younger Dryas also suggest that deepwater production decreased [*Hughen et al.*, 1998, 2004]. Decreasing NADW formation in ocean circulation models reduces the Atlantic's cross-equatorial heat transport, cooling the North Atlantic and warming the southern subtropical Atlantic [*Manabe and Stouffer*, 1997; *Vellinga and Wood*, 2002]. Some western tropical Atlantic paleoceanographic records do show warming during these events [*Ruhlemann et al.*, 1999]. Some Antarctic ice core records also imply that the Southern Hemisphere expression of deglacial climate changes were antiphased with Northern Hemisphere changes. An Antarctic Cold Reversal (ACR) preceded the Greenland Younger Dryas cool interval, during which Antarctica warmed [*Blunier et al.*, 1998]. This "bipolar seesaw" pattern is not borne out in other Antarctic records, however, which suggest synchronous climate changes at both poles during the last deglaciation [*Steig et al.*, 1998; *Pahnke et al.*, 2003]. Deglacial climate records from many locations around the globe also show cool intervals during the Younger Dryas rather than the earlier Antarctic Cold Reversal period; however, few records have been published from the South Atlantic [*Broecker*, 2003].

[6] One relatively high-resolution study of southern tropical Atlantic SSTs based on alkenone unsaturation ratios in GeoB1023-5 suggests that SSTs cooled during the Younger Dryas but warmed during Heinrich event 1 (H1), which the authors interpret as evidence that the mechanisms for these two events were quite different [*Kim et al.*, 2002]. The authors attribute the Younger Dryas cooling to enhanced upwelling, which may have overwhelmed any circulation-induced warming. The record also does not show any upwelling-induced cooling during the early to middle Holocene at 6–9 ka, when *McIntyre and Molfino* [1996] found deepening of the equatorial Atlantic thermocline similar to that seen during Heinrich events. However, alkenone-based SST reconstructions from ODP1078C, a site just north of GeoB1023-5 on the other side of the Angola-Beguela front (ABF), do indicate a somewhat cooler interval during the early to middle Holocene [*Kim et al.*, 2003]. In modern climate, the SST difference across the ABF is proportional to the strength of the zonal component of SE trade winds. ODP1078C records suggest that this SST gradient was weaker during the Bølling-Alleröd and the early to middle Holocene. This is consistent with either weaker or more meridional SE trade winds during these times, as proposed by *McIntyre and Molfino* [1996]. A comparison with an alkenone-derived SST record from the western side of the basin found similar results [*Kim and Schneider*, 2003].

[7] Planktonic foraminiferal faunal abundance data from Hole 658C within an upwelling region off NW Africa in the subtropical North Atlantic also indicate significantly cooler intervals during the mid-Holocene [*deMenocal et al.*, 2000a], whereas the alkenone-derived SST record did not [*Zhao et al.*, 2000]. Discrepancies between these records may be due to seasonal differences in the temperature recorded by different proxies [*Chapman et al.*, 1996], or by sediment resuspension and refocusing. Offsets between radiocarbon ages of alkenone molecules and shells of planktonic foraminifera imply that resuspension of fine sediments or some other factor may be confounding alkenone paleoclimate signals in sites with high rates of accumulation [*Ohkouchi et al.*, 2002; *Mollenhauer et al.*, 2003].

[8] Perhaps the *Kim et al.* [2002] alkenone record lacks the mid-Holocene cool intervals seen in the *deMenocal et al.* [2000a] record simply because the associated changes in atmospheric circulation were absent in the Southern Hemisphere tropics. Northern subtropical cool intervals off NW Africa have been attributed to enhanced precessional forcing of monsoon winds and regional upwelling [*Mix et al.*, 1986; *deMenocal et al.*, 2000b]. Perhaps these feedbacks did not affect the Southern Hemisphere. Productivity proxies in several cores from ODP Leg 175 off the coast of Namibia in the southeastern Atlantic, however, document increased upwelling during glacial periods [*Berger and Wefer*, 2002]. Perhaps the mid-Holocene changes in atmospheric circulation were manifested as increasing meridionality rather than weakening of the SE trade winds, as the history of the SST gradient across the Angola-Benguela front suggests [*Kim et al.*, 2003]. Relatively low-resolution alkenone paleotemperatures and planktonic foraminiferal oxygen isotope ratios from a site closer to the Benguela coastal upwelling zone do indicate cooler intervals in the early to middle Holocene, however [*Mollenhauer et al.*, 2003]. Increased thermocline depth in the western tropical Atlantic during this time also suggests that these mid-Holocene shifts in atmospheric circulation were widespread, but this thermocline deepening was more likely due to increased zonality of the trade winds rather than increased meridionality [*Arz et al.*, 2001]. What can temperature reconstructions from a different paleoclimate proxy, Mg/Ca in planktonic foraminifera, say about low-latitude South Atlantic climate changes in the Holocene and last deglacial period?

2. Study Area

[9] We analyzed Holocene and last deglacial sediment samples in sections 1 and 2 of Core 1H from Ocean Drilling Program (ODP) Leg 175 Hole 1084B because of its high

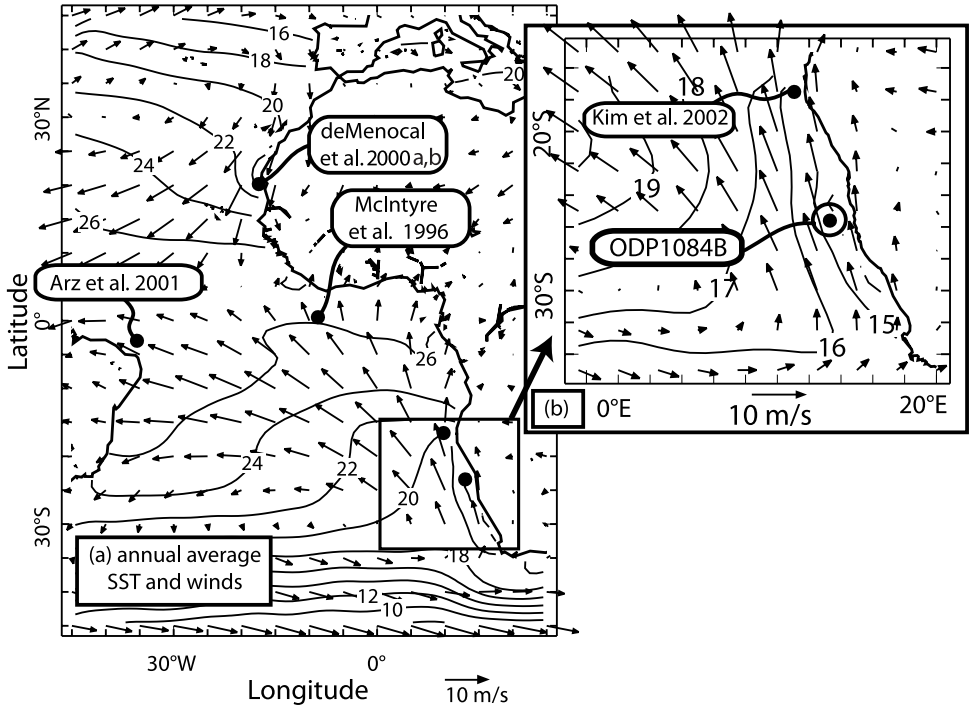

Figure 1. (a) Map of the tropical Atlantic showing the location of several paleoclimatic records discussed in the text. Arrows show National Centers for Environmental Prediction/National Center for Atmospheric Research reanalysis [*Kalnay et al.*, 1996] mean annual wind strength and direction (scale gives 10 m/s arrow), contours show NOAA World Ocean Atlas sea surface temperatures [*Conkright et al.*, 1998]. (b) Inset shows close-up of Hole 1084B location, with average of peak upwelling season (September–October–November) wind and SST values.

rates of sediment accumulation (up to 26 cm/ka) and its location on the edge of the most intense coastal upwelling cell off the southwestern coast of the African continent. The planktonic foraminifera preserved in Hole 1084B sediments record past changes in surface ocean temperatures in this location, which are greatly influenced by changes in upwelling rates because of changes in trade wind strength and direction.

2.1. Modern Oceanographic Setting

[10] Hole 1084B was drilled at 25°30.83′S, 13°1.67′E, at 1992 m water depth, about 300 km off the coast of Namibia over the continental slope in the Northern Cape Basin (Figure 1). The Benguela region has been differentiated into the Northern Benguela Region (NBR) and the Southern Benguela Region (SBR), with their boundary at 26°–27°S. The SBR is characterized by a stronger seasonal upwelling cycle that peaks in Southern Hemisphere summer, while the NBR, where Hole 1084B is located, has a weaker seasonal upwelling cycle that peaks in August–October (Southern Hemisphere winter-spring) but maintains stronger year-round upwelling [*Bubnov and Kostianoy*, 2001].

[11] The seasonal SST cycle at the location of Hole 1084B is dominated by the upwelling of cooler South Atlantic Central Water (SACW). This mode water forms in the South Atlantic Convergence Zone and extends as far north as 15°N below the surface [*Lutjeharms and Meeuwis*, 1987; *Poole and Tomczak*, 1999]. Water mass analysis shows that the SACW is moving southward along the continental shelf in subsurface currents when it is upwelled [*Gordon et al.*, 1995]. Maximum SSTs of 17.2°C occur in Southern Hemisphere fall (February–April), whereas minimum SSTs of 14.8°C occur in Southern Hemisphere spring (September) [*Conkright et al.*, 2002] (accessed in 2004). Hole 1084B is located on the edge of the "permanent" (year-round) upwelling zone, well within the extent of "filamentous" (intermittent) upwelling [*Iita et al.*, 2001]. The local region of upwelling where Hole 1084B is located is known as the Luderitz cell, which has the strongest year-round upwelling of any of the coastal upwelling cells in the Benguela current region. This cell extends farther offshore (~380 km on average) than any of the other cells [*Lutjeharms and Meeuwis*, 1987]. The Benguela Current region is unusual among coastal upwelling zones because warmer waters are located both to the north and to the south, as Indian Ocean waters enter the South Atlantic through the Agulhas retroflection.

2.2. Modern Foraminiferal Ecology

[12] A study of 140 grab samples and core tops shows that the area in which Hole 1084B is located is dominated by four species of planktonic foraminifera: *Globorotalia inflata*, *Neogloboquadrina pachyderma* (right coiling), *N. pachyderma* (left coiling), and *Globigerina bulloides*, which account for ~83% of total planktonic foraminifera abundance on average [*Giraudeau*, 1993; *Giraudeau and Rogers*, 1994]. In the style of *Imbrie and Kipp* [1971]

transfer function analysis, three foraminiferal assemblages account for >95% of the total foraminiferal relative abundance variations in this region.

[13] In many other areas of upwelling around the world, the core of the upwelling region is dominated by *G. bulloides*, a transitional to polar species [*Prell and Curry*, 1981; *Gupta et al.*, 2003]. The core Benguela upwelling region (a narrow strip along the shore with SSTs less than 16°C), however, is dominated by *N. pachyderma* (left), a polar species. Outside this coastal strip north of ~30°S lies an assemblage dominated by *G. bulloides* and *N. pachyderma* (right), another transitional to polar species. This assemblage is characterized as an ''indicator for intermediate conditions between [the] warm oligotrophic offshore environment and cool upwelled coastal waters'' [*Giraudeau and Rogers*, 1994]. The area outside this coastal strip south of ~27°S is dominated by a similar intermediate assemblage composed almost entirely of *G. inflata*, a transitional species which is associated with the Benguela Current in regions of reduced upwelling. In modern Holocene conditions, the Hole 1084B site lies well within the area of the *N. pachyderma* (right) and *G. bulloides* assemblage, at least 0.5° longitude west of the boundary with the coastal assemblage. Therefore increases in the percentage of *N. pachyderma* (left) in older Hole 1084B sediments should indicate extension westward of the region dominated by this species and intensification of the upwelling.

[14] Sediment trap results from a nearby location in Walvis Bay confirm that fluxes of *N. pachyderma* (left) and *G. bulloides* to the sediments increase when regional winds strengthen and become more southerly in October and November [*Giraudeau et al.*, 2000]. As the winds become stronger and more parallel to the coastline, upwelling rates increase, decreasing the local SST and creating favorable conditions for these two species. The relative abundance of *N. pachyderma* (left) as a percentage of all species also peaks during the periods of strongest, most southerly winds and lowest local SST.

3. Materials and Methods

[15] Samples of Hole 1084B sediments were obtained from the ODP repository in Bremen, Germany. After being shaken for 2 hours in a surfactant solution of sodium metaphosphate, with 3% hydrogen peroxide added to denature any organic material remaining from the high organic content of the upwelling zone sediments, samples were washed through 150 micron sieves with deionized water and dried in a 50°C oven. Low foraminiferal abundances precluded selecting *G. bulloides* from only narrow size fractions, so specimens of *G. bulloides* were picked from the >150 μm fraction and *G. bulloides* Mg/Ca measurements were performed every 1 cm between 0 and 352 cm. Planktonic faunal abundances were counted every other centimeter, except for 0–31 cm when they were counted every centimeter, and 283–353 cm where they were counted every 4 cm. On the basis of photographs of the core in the ODP archives, a core void between 98 and 102 cm was assumed to have been caused by gas expansion and separation of continuous sediment layers. Depths were adjusted accordingly: The ''98 cm'' reported by ODP is 98 cm here, whereas ''102 cm'' is 99 cm, ''103 cm'' is 100 cm, etc. On the basis of shipboard core descriptions, the ''core top'' of Core 1H was assumed to lie at a depth of 5 cm as labeled by ODP. (We did not convert ''meters below seafloor'' depths to ''meters composite depth,'' but these can be obtained by adding 0.09 m to all depths reported here (Ocean Drilling Program, Hole/core summary, accessed 2004, available at http://iodp.tamu.edu/janusweb/coring_summaries/holesumm.cgi).)

3.1. Radiocarbon Dating

[16] Fifteen radiocarbon dates were measured at the Lawrence Livermore National Laboratory Center for Accelerator Mass Spectrometry on monospecific samples of planktonic foraminifer *G. bulloides*, eight in Holocene sediments and seven in sediments from the last glacial maximum and deglacial period (Table 1). Conversion to calendar years was performed with CALIB 4.3, using probability-based Method B [*Stuiver and Reimer*, 1993]. On the basis of estimates by *Southon et al.* [2002], a constant local offset of 230 ± 50 (ΔR) to the global reservoir correction of 400 years was used [*Southon et al.*, 2002]. This is the best available approximation, although the reservoir age can vary locally, and can change substantially through time, especially in an upwelling area, as demonstrated by *Staubwasser et al.* [2002]. To construct the best Holocene and last deglacial chronology at Hole 1084B, the dates were interpolated linearly in the minimum number of segments (whose endpoints are footnoted in Table 1 in the interpolated ages column) such that all interpolated dates fall within the 2-σ confidence intervals (Figure 2a). The younger end of the 2-σ confidence interval of the oldest date was used to force the best possible match in the interval of Heinrich event 1. For an estimate of the uncertainty inherent in this chronology, the average length of the 1-σ confidence interval in the Holocene was 280 years, the average 2-σ interval in the Holocene was 510; in the Last Glacial Maximum and deglacial period these intervals were 910 and 1480 years.

3.2. Faunal and Mg/Ca Data Collection

[17] The four dominant species of planktonic foraminifera were counted in a random subsample of 150–200 individuals; all other species were counted as ''other'' and each dominant species' relative abundance calculated as a percentage of the total number counted. Replicate counting precision was estimated by recounting six samples 2–3 times each: The average difference between the repeated relative abundance measurements was 3%, or a relative standard deviation (RSD) of 16.9%. Seventy individual *G. bulloides* individuals from each sample depth were lightly crushed and cleaned with oxidative and reductive reactions according to methods outlined by *Boyle and Keigwin* [1985] and *Boyle and Rosenthal* [1996], with the exception of the final weak acid rinse which was not conducted. Owing to the relatively thin tests of this species, initial preparations including this step dissolved the samples entirely.

[18] Mg/Ca ratios of the dissolved samples were measured on a Jobin Yvon inductively coupled plasma atomic

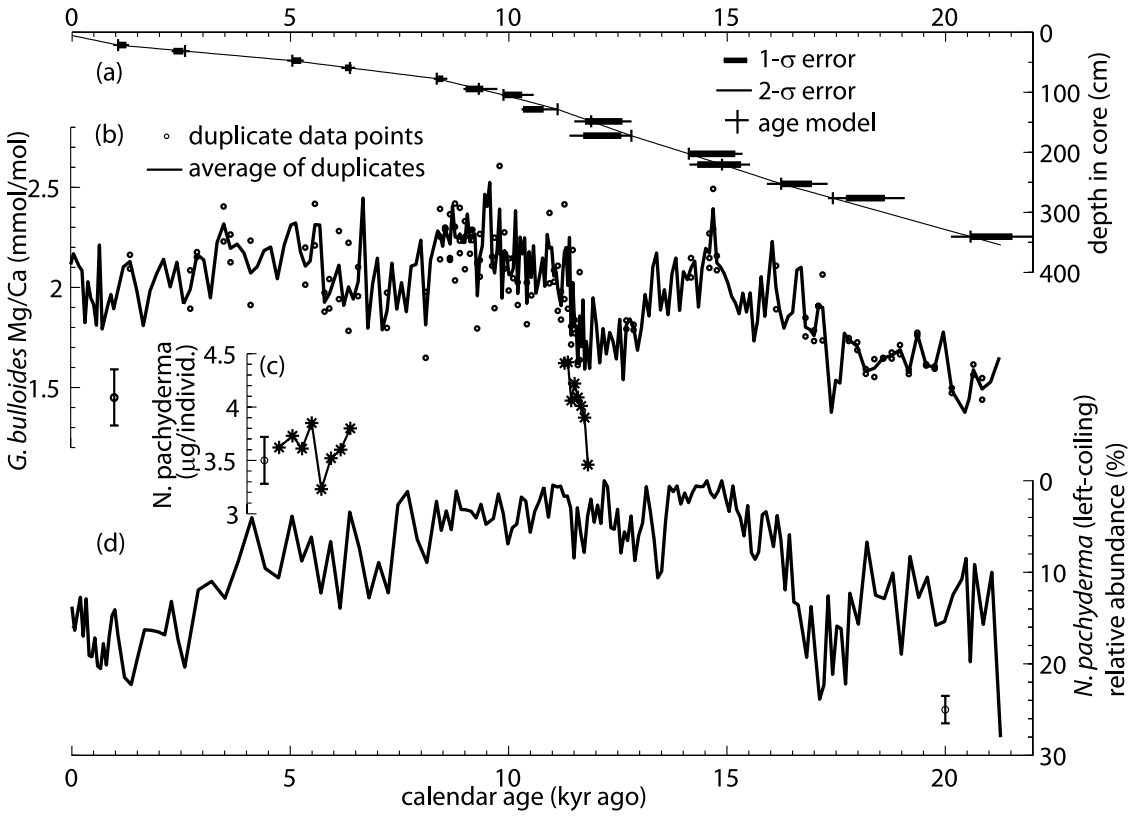

Figure 2. (a) Radiocarbon ages (calendar years) measured at various sample depths, shown with 1-σ and 2-σ confidence intervals and the linearly interpolated age model constructed from these dates. (b) Hole 1084B *G. bulloides* Mg/Ca (mmol/mol). Circles show individual duplicate and triplicate measurements; line shows average of all replicates, ±0.6°C sampling error (bottom left) estimated from pooled standard deviation of all replicate measurements. (c) Size-normalized weights of *N. pachyderma* (right coiling) as a test for the influence of dissolution. (d) Relative abundance (%) of *N. pachyderma* (left coiling) on inverted scale because larger proportion of this species and lower values of *G. bulloides* Mg/Ca both indicate increased upwelling intensity at Hole 1084B, ±3% sampling error estimated from several recounts.

emission spectrophotometer (ICP-AES) with a Gilson autosampler. A total of 300 measurements were made, including 70 duplicates and 8 triplicates, in which additional *G. bulloides* were picked separately from the same sediment sample and prepared identically. The raw data were drift corrected as described by *Schrag* [1999]; however, we used the 317 nm, 279 nm, and 407 nm emission lines for Ca, Mg, and Sr, respectively because calibration linearity was optimal over the measured concentration ranges. Within-run measurement stability averaged between 0.2 and 0.4% based on the relative standard deviation (RSD) of many repeated measurements of a known laboratory standard. Over three years, the long-term reproducibility of hundreds of analyses of an in-house consistency standard was 1.4% RSD.

[19] Molar elemental ratios were converted to SSTs using the *G. bulloides* calibration of *Mashiotta et al.* [1999]:

$$T(^{\circ}C) = (\log([Mg]/[Ca]/0.474))/0.107$$

This calibration was chosen because it extends the *Lea et al.* [1999] culture calibration to the lower temperatures more characteristic of our study area, by including some south Atlantic core top values. We estimate our sampling precision by calculating the pooled standard deviation of all duplicate and triplicate measurements. This value of 0.14 mmol/mol, or an RSD of 6.8%, is comparable to the reproducibility of at least one other high-quality planktonic Mg/Ca data set [*Lea et al.*, 2003]. Slightly better reproducibility of another Mg/Ca study from our lab by *Koutavas et al.* [2002] may be due to its more pelagic location, constrained size fraction analyses, or the selection of replicate sample mass from the same pool of crushed individual foraminifera. Sampling errors from all studies typically dwarf the analytical errors, as ours does by almost an order of magnitude. However, the corresponding temperature uncertainty of ±0.6°C (see representative error bar in lower left of Figure 2b, lower right of Figure 3c, and lower right of Figure 4c) is still less than the ±1.1°C reported error in the temperature calibration [*Mashiotta et al.*, 1999].

[20] Although Mg/Ca paleothermometry is not known to be affected by ice volume changes as are oxygen isotopic ratios, overprinting by dissolution remains a problem.

Table 1. Radiocarbon Data From Hole 1084B

CAMS ID[a]	Hole[b]	Core[c]	Section[d]	Depth in Section,[e] m	Center Depth Below Seafloor,[f] m	Age,[g] ^{14}C years B.P.	Plus/Minus,[h] ^{14}C years	Calendar Age 1-σ Error Bounds[i]		Calendar Age 2-σ Error Bounds[j]		Interpolated Age, calendar years B.P.	Average Sediment Rate,[k] cm/kyr	Average Time Step,[l] yrs/cm
								Lower	Upper	Lower	Upper			
85026	1084B	1H	1	21	0.215	1,820	95	1,244	1,053	1,303	946	1,053[m]		
85027	1084B	1H	1	31	0.315	2,950	79	2,547	2,321	2,696	2,279	2,588		
85028	1084B	1H	1	47	0.475	5,070	68	5,248	5,043	5,303	4,928	5,043[m]	6.5	153
85029	1084B	1H	1	59	0.595	6,130	79	6,400	6,247	6,481	6,166	6,365		
85030	1084B	1H	1	77	0.775	8,195	71	8,497	8,349	8,592	8,282	8,349[m]	9.1	110
85031	1084B	1H	1	93	0.945	8,935	71	9,416	9,011	9,739	8,960	9,312		
85032	1084B	1H	1	107	1.045	9,715	68	10,307	9,879	10,569	9,833	9,879[m]	17.6	57
85033	1084B	1H	1	131	1.285	10,040	79	10,797	10,322	11,117	10,291	11,117[m]	19.4	52
85034	1084B	1H	2	1	1.485	11,040	103	12,603	11,745	12,808	11,499	11,884		
85035	1084B	1H	2	25	1.725	10,990	112	12,576	11,702	12,804	11,389	12,804[m]	26.1	38
85036	1084B	1H	2	55	2.025	13,105	71	15,185	14,139	15,351	14,120	14,120[m]	22.8	44
85037	1084B	1H	2	73	2.205	13,240	158	15,317	14,311	15,523	14,134	14,881		
85038	1084B	1H	2	105	2.525	14,550	236	16,939	16,235	17,298	15,908	16,235[m]	23.6	42
90228	1084B	1H	2	129	2.765	15,920	314	18,610	17,717	19,064	17,309	17,418		
90229	1084B	1H	3	43	3.405	18,430	314	21,531	20,572	22,014	20,121	20,572[m]	20.3	49

[a]Lawrence Livermore National Laboratory Center for Accelerator Mass Spectrometry identification (ID) number.
[b]ODP Hole ID (all 1084B).
[c]ODP Core ID (all 1H).
[d]ODP section ID.
[e]Depth in section (cm) of top of each sample.
[f]Depth below seafloor in center of sample, corrected for voids as noted in text.
[g]Age in radiocarbon years.
[h]One-sigma error in radiocarbon age.
[i]Lower and upper 1-σ limits on calendar ages using probability method of calculating intercepts.
[j]Lower and upper 2-σ limits on calendar ages using probability method of calculating intercepts.
[k]Average sedimentation rates.
[l]Average time steps in each interpolated interval (boxes indicate interpolated intervals).
[m]Endpoints of interpolated intervals (see text for discussion).

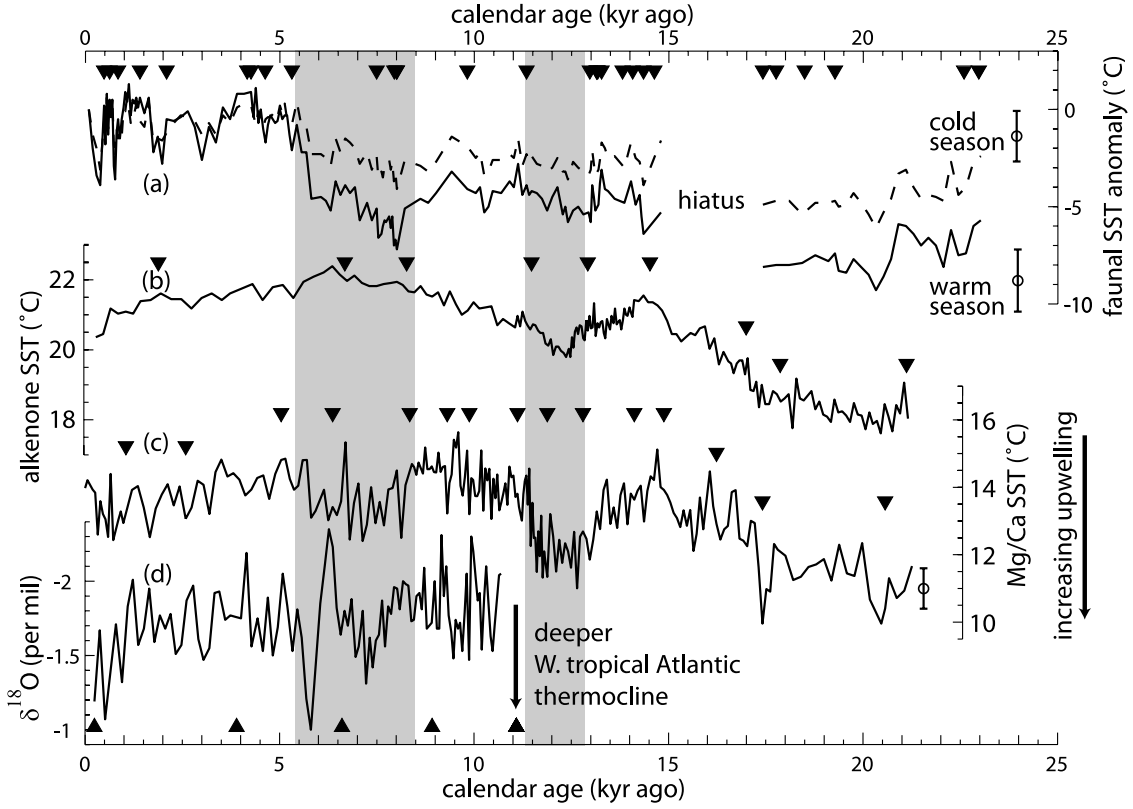

Figure 3. Several tropical Atlantic paleoceanographic records: (a) cold and warm season sea surface temperature (SST) anomalies derived from relative faunal abundances in ODP658C in the NE tropical Atlantic [*deMenocal et al.*, 2000a]; (b) alkenone-based SST estimates from GeoB1023-5 just north of the Walvis Ridge in the SE tropical Atlantic [*Kim et al.*, 2002]; (c) Hole 1084B SST estimated from *G. bulloides* Mg/Ca; and (d) difference in $\delta^{18}O$ (per mil versus Peedee belemnite) between surface-dwelling *G. sacculifer* and deeper-dwelling *G. tumida* in GeoB 3910-2 off the coast of Brazil in the NW tropical Atlantic [*Arz et al.*, 2001], scale inverted so that deeper thermocline values can be more easily compared to increased upwelling values on other graphs. Triangles indicate radiocarbon dates in each record.

Studies have shown that dissolution tends to preferentially remove the higher-Mg pregametogenic calcite [*Elderfield and Ganssen*, 2000; *Dekens et al.*, 2002; *Rosenthal and Lohmann*, 2002]. A limited test for the influence of dissolution in ODP1084 was conducted over two depth intervals in the record, in order to see if the changes in Mg/Ca seen in these periods should be attributed to changes in dissolution rather than changes in temperature. Every 2 cm between 45–59 cm and 132–149 cm, the average weight of 40 individuals of *N. pachyderma* (right) from the 150–250 μm size fraction was normalized by their average diameter, which was measured optically for each individual. This removes the variation of weight based on size variability alone. *G. bulloides* was not available for this investigation, as most individuals had been consumed by the Mg/Ca analyses. When dissolution has thinned the calcium carbonate shells, the average weight should be lower and should shift proportionally to changes in Mg/Ca values if dissolution is the leading cause for the observed SST variations in the Hole 1084 Mg/Ca record. Lack of apparent correlation between Mg/Ca values and *N. pachyderma* (right) weights would suggest that these shifts in Mg/Ca values are representative of surface ocean conditions and are not primarily due to the influence of dissolution.

4. Results

4.1. Chronology

[21] The age model constructed from the 15 radiocarbon dates on monospecific samples of *G. bulloides* indicates variable sediment accumulation rates over the last 21,000 years in Hole 1084B (Table 1, average sedimentation rates column, and Figure 2a). Highest rates of ~18–26 cm/kyr occurred in the Last Glacial Maximum (LGM), deglacial, and early Holocene (~9–21 ka). Accumulation rates were lower (~9–17 cm/kyr) in the early to middle Holocene (~5–9 ka). The lowest rates in this section of Hole 1084B (~6 cm/kyr) occurred in the late Holocene (~0–5 ka). Average sampling resolution was 100 years, ranging between 40 and 290 years.

4.2. Faunal Abundances and Mg/Ca Ratios

[22] The core top values of both the faunal abundance and Mg/Ca data are consistent with known modern conditions

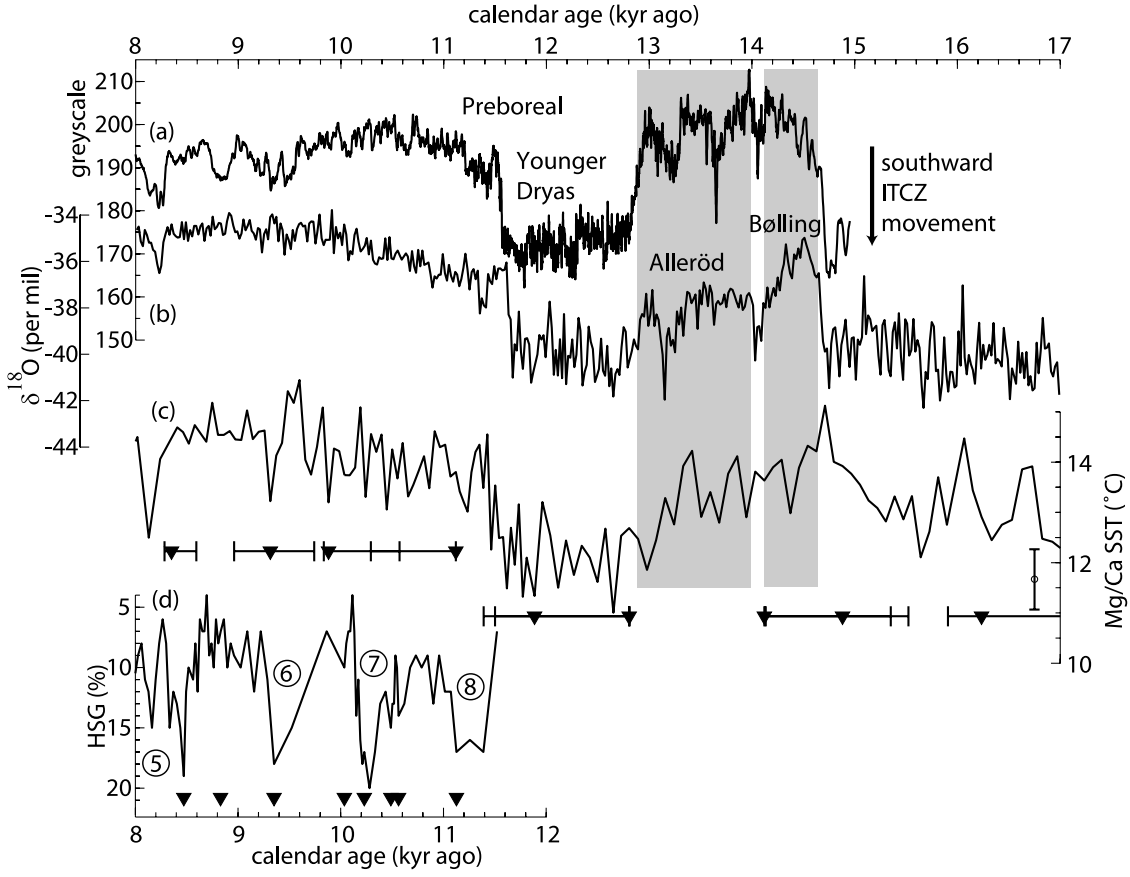

Figure 4. Two high-resolution paleoclimatic records of the end of the last glacial period: (a) Cariaco Basin PL07-58PC sediment grayscale [*Hughen et al.*, 2000], where darker sediments indicate more terrestrial runoff associated with higher rainfall of Intertropical Convergence Zone (ITCZ) in more northerly position, and (b) Greenland Ice Sheet Project 2 ice $\delta^{18}O$ (per mil versus standard mean ocean water) [*Stuiver and Grootes*, 2000] where lighter (more negative) values indicate colder Greenland temperatures. The ITCZ seems to have moved southward as Greenland cooled during the Younger Dryas, brief events that punctuated the Bølling-Alleröd period, the Preboreal ~11.3 ka, and a distinct event in the early Holocene ~8.2 ka; many of these features are seen in the (c) Hole 1084B Mg/Ca temperature record (2-σ confidence intervals indicated with each radiocarbon date, shown by triangles). By contrast, few of the significant ice-rafting events (circled numbers) seen in the (d) North Atlantic early Holocene hematite-stained grain record from MC52/VM29-191 [*Bond et al.*, 2001] are seen in the Hole 1084B temperature record.

(Figures 2b and 2d). Within our counting error of 3%, the 14% *N. pachyderma* (left) abundance counted in the most recent sediments matches values of 18% counted in several surface sediment samples from this area in a regional calibration study [*Giraudeau*, 1993]. The "core top" Mg/Ca molar ratio value of 2.1 mmol/mol corresponds to a temperature of 14.0°C using the *Mashiotta et al.* [1999] calibration. This matches, within the ±1.1°C confidence limits of the calibration equation, the modern winter (upwelling season) SST of 14.8°C reported in the 1998 NOAA World Ocean Atlas (WOA98) (accessed in 2004) [*Conkright et al.*, 1998] for the 1° latitude by 1° longitude grid square in which the core is located.

[23] On the basis of the sediment trap data showing peak growth of *G. bulloides* during the most intense upwelling periods in Southern Hemisphere winter and spring [*Giraudeau et al.*, 2000], it is not surprising that *G. bulloides* are recording a slightly lower temperature than the actual seasonal average SST. This may also be because some individuals of this species are found as far down as the thermocline, although most individuals live in the mixed layer of the upper ocean [*Oberhansli et al.*, 1992; *Boltovskoy et al.*, 2000]. The slight offset may also be due to preferential removal of high-Mg primary calcite by postdepositional dissolution [*Elderfield and Ganssen*, 2000; *Dekens et al.*, 2002; *Rosenthal and Lohmann*, 2002].

[24] The overall trends in both the Mg/Ca and faunal abundance data sets are encouragingly similar over the last 21,000 years, although there are some notable differences. In general, when the Mg/Ca values are low, indicating cooler SSTs, the *N. pachyderma* (left) percentages (hereafter NPS%) are high (Figures 2b and 2d), indicating

greater upwelling. The highest average NPS% (18.4%) and the lowest average Mg/Ca molar ratios (1.7 mmol/mol) occurred between 17.0 and 18.0 kyr ago (ka) in the LGM (Figure 2). When the Mg/Ca molar ratios are converted to temperatures based on the *Mashiotta et al.* [1999] calibration, average LGM SST for this period is estimated at 11.8°C. Between 15.0 and 13.0 ka in the Bølling-Alleröd period, average NPS% fell to almost zero and Mg/Ca SSTs rose to 13.7°C. In the Younger Dryas period between 11.5 and 13.0 ka, Mg/Ca fell to an average of 1.8 mmol/mol (12.2°C SST) and NPS% rose to an average of 4.8%. The highest Mg/Ca value in the entire record, 2.5 mmol/mol (equivalent to 15.4°C SST), occurred in the mid-Holocene at 9.5 ka. The mid-Holocene between 8.4 and 5.8 ka was marked by low average Mg/Ca values of 2.0 mmol/mol (13.5°C SST), followed by a period of warmer SSTs between 5.8 and 3.4 ka. NPS% then rose sharply between 3.4 and 1.0 ka, while Mg/Ca fell to 2.0 mmol/mol (13.6°C SST). Lowest average Holocene Mg/Ca values of 1.9 mmol/mol and highest average NPS% values of 17.5% occurred between 1 and 0.3 ka. Since 0.3 ka, values have been essentially constant at modern conditions.

[25] There are some prominent differences between the Mg/Ca and the faunal abundance data sets, however. High-frequency variability in the two records shows little similarity. Decreases in Mg/Ca during the Younger Dryas interval are much more prominent than increases in NPS%. The increases since the mid-Holocene in NPS% are much greater than the decreases of Mg/Ca: Magnitudes of NPS% during the last 3,000 years are comparable to those of the interval between 17.0 and 18.0 ka. The interval of increased NPS% between 17.0 and 18.0 ka is much longer than the interval of lowered Mg/Ca during that same period.

4.3. Influence of Dissolution

[26] The size-normalized *N. pachyderma* weights (Figure 2c) suggest that there is very little influence of dissolution on the mid-Holocene Mg/Ca shifts between 4.7 and 6.4 ka, but they do not rule out some influence on the Mg/Ca data between 11.0 and 11.7 ka at the end of the Younger Dryas (Figure 2c). The weight values do not change very significantly in the mid-Holocene compared with the ±0.44 μg error bars; neither do they change consistently with the Mg/Ca values: The correlation coefficient is −0.39 (α = 0.2, N = 8). If these changes in weight were due to dissolution-related changes in shell thickness that lowered Mg content, this correlation should be positive. Between 11.0–11.7 ka, the shift in weight values is almost twice the range of the mid-Holocene values, which implies that there may be some influence of dissolution on the shell weights. The weight values and Mg/Ca values have a correlation coefficient of 0.69 (α = 0.2, N = 8): This suggests that dissolution might account for up to half of the Mg/Ca shift at the end of the Younger Dryas.

[27] *Rosenthal and Lohmann* [2002] estimated the rates of planktonic foraminifera shell thinning due to dissolution by measuring the size-normalized shell weights and Mg/Ca in two species from a core top transect on the Sierra Leone Rise. They estimate that *G. sacculifer* are only reduced by 0.03 mmol/mol Mg/Ca per μg of size-normalized weight loss, while *G. ruber* are reduced by 0.38 mmol/mol for every μg of weight loss [*Rosenthal and Lohmann*, 2002]. *G. bulloides* is probably affected by dissolution somewhere in this range, so the 0.95 μg shift in shell weights at the end of the Younger Dryas may mean that between 0.03 and 0.38 mmol/mol of the shift in Mg/Ca is potentially attributable to dissolution. This corresponds to a temperature shift of 0.15–1.8°C at 13°C. So the apparent LGM-early Holocene temperature difference of 4.8°C may only be 3°–4.6°C.

5. Discussion

[28] Shifts in Mg/Ca–based SST at the Hole 1084B site are likely to be related to changes in upwelling intensity, because of its location on the border of the strongest upwelling cell on the southwestern coast of the African continent. Other potential controls on SST at this site cannot be ruled out on the basis of this data set alone, however. Temperature changes in the source region of the upwelled water are indistinguishable from temperature changes because of fluctuations in upwelling intensity. Variations in temperature of the Benguela Current, as well as changes in rates of advection, undoubtedly also influence SST at the ODP1084B site. Changes in the seasonality of the upwelling cannot be determined from this data set either. These factors may account for some of the differences between the Mg/Ca record and the abundance of *N. pachyderma* (left). The apparent amplification of the Mg/Ca shift during the Younger Dryas by selective dissolution may account for some of the lack of agreement in this interval as well. Other factors which might affect faunal abundance, and therefore account for some of the differences between these two records, include nutrient availability, competition between species, and other ecological pressures.

[29] All of the factors affecting SST at the Hole 1084B site have common roots in climate-mediated atmospheric and oceanic processes, however. Consistent climate patterns begin to emerge when the Mg/Ca–based temperature record from ODP1084B is compared with other high-resolution tropical Atlantic paleoclimate records. These comparisons depend on accurate timescales for all records, however, and secular variations in marine radiocarbon reservoir ages are likely at the Hole 1084B site because of changes in upwelling rates. All the comparisons made here would be greatly strengthened by a construction of a detailed chronology of marine radiocarbon reservoir ages in the Benguela upwelling region.

5.1. Younger Dryas and Bølling-Alleröd

[30] This data set corroborates the *Kim et al.* [2002] alkenone evidence of cooling in the southern subtropical Atlantic during the Younger Dryas period. The existence of radiocarbon dating offsets between measurements made on foraminiferal calcite, total organic carbon, alkenone molecules, and fine fraction sediments in some locations complicates the interpretation of alkenone-derived SST records [*Ohkouchi et al.*, 2002]. Local evidence for offsets of 1–2.5 kyr between dates of planktonic foraminifera and

alkenone molecules in the last 16 kyr [*Mollenhauer et al.*, 2003] specifically challenges the fidelity of high-resolution alkenone records documenting century-millennial-scale SST variability. However, the Hole 1084B SST record indicates cooler temperatures during the same interval as the most substantial and most abruptly manifested cool interval in the *Kim et al.* [2002] study, between 11.5 and 13.0 ka (see Figure 3b and 3c). This is consistent with the timing of the Younger Dryas, the deglacial cold reversal seen in many locations in the Northern Hemisphere such as ice cores in Greenland [*Stuiver and Grootes*, 2000] (see Figure 4b), rather than the earlier Antarctic Cold Reversal seen in some Antarctic ice cores between 12 and 15 ka. Notably, the Mg/Ca SST record documents the characteristically abrupt (century scale) onset and termination of the Younger Dryas cooling event [*Alley et al.*, 1993], whereas these transitions are more gradual in the alkenone record.

[31] Several geochemical signals in Cariaco Basin sediments that record precipitation in northern Brazil, including spectral reflectance and percentage of Ti, also shift substantially during the Younger Dryas (see Figure 4a). These shifts have been attributed to lower terrestrial runoff because of decreased precipitation associated with southward movement of the mean position of the Intertropical Convergence Zone (ITCZ) [*Hughen et al.*, 2000; *Peterson et al.*, 2000; *Haug et al.*, 2001]. Amplifying the sediment color change associated with southward movement of the ITCZ is an increase in lighter colored sediments from higher productivity due to increased coastal upwelling as the NE trade winds reach farther south. Greater trade-wind-driven upwelling in the Cariaco Basin during the Younger Dryas has been corroborated by Mg/Ca analyses of the planktonic foraminifer *Globigerinoides ruber* (white) [*Lea et al.*, 2003].

[32] Even after taking into account an estimate of the possible effects of dissolution on Hole 1084B Mg/Ca concentrations, the magnitude of the temperature change between the peak of the Younger Dryas cool interval and the early Holocene is consistent between the Hole 1084B and *Kim et al.* [2002] alkenone records. Given all uncertainties, both records suggest temperatures during the Younger Dryas were cooler by 2°–3°C. Both records also suggest temperature changes of 4°–5°C between the LGM and early Holocene thermal maximum. Noble gas concentrations and oxygen isotopes in groundwater at Stampriet in central Namibia indicate 5.3°C cooler LGM temperatures [*Stute and Talma*, 1998]. Terrestrial temperatures probably changed more than ocean temperatures: Estimates of LGM-present temperature change in Brazil based on groundwater noble gases found a similar temperature difference of 5.4°C [*Stute et al.*, 1995].

[33] Comparison of the Hole 1084B Mg/Ca temperature record with the much higher resolution Greenland and Cariaco Basin records is also striking for the Bølling-Alleröd Warm period (BA) that preceded the Younger Dryas (see Figures 4a, 4b, and 4c). To illustrate the uncertainty associated with the conversion to calendar years in the Hole 1084B age model, the 2-σ error intervals associated with each radiocarbon date are plotted in Figure 3c. Considered within the context of this uncertainty in the timescale, the pattern of smaller oscillations within the BA and their relative amplitudes are similar in all the records. The warmest period in the ODP1084b record (and northernmost ITCZ in Cariaco Basin grayscale records) occurred early in the Bølling, followed by cooler intervals (and southward displacement of the ITCZ), and then two warm (northern ITCZ displacement) peaks in the Alleröd of similar magnitude separated by a larger cool interval (southern ITCZ displacement). The ''Preboreal'' oscillation that is evident in the two high-resolution records at 11.4 ka may also be apparent in the ODP1084 record at 11.2 ka, although this 0.9°–1.2°C shift is only marginally greater than the analytical uncertainty as estimated by the ±0.6°C reproducibility of the data set. The oscillation is resolved throughout several individual data points, however.

5.2. Holocene

[34] With the exception of the mid-Holocene return to conditions similar to those of the Younger Dryas (~8.4–5.8 ka), the Hole 1084B Mg/Ca temperatures show an overall gradual cooling trend throughout the Holocene from a peak ~9.5 ka (Figure 3c). Other than the slightly later peak warming in the *Kim et al.* [2002] alkenone record (Figure 3b), the overall temporal patterns in the two records are quite similar. This agrees with the characterization of the early Holocene ''Thermal Maximum'' in the Cariaco Basin [*Haug et al.*, 2001], Barents Sea [*Duplessy et al.*, 2001], Norwegian Sea [*Birks and Koc*, 2002], and in glacial advances in Iceland [*Stotter et al.*, 1999]. It is earlier, however, than the Holocene ''Optimum'' seen from 4–6 ka in boreholes in the Ural mountains [*Demezhko and Shchapov*, 2001], in vegetation changes on Iturup Island in the northwestern Pacific [*Razjigaeva et al.*, 2002], and in the SSTs off northwest Africa [*deMenocal et al.*, 2000a] (Figure 3a).

[35] These offset Holocene temperature trends are consistent with a coupled ocean-atmosphere model study that projected the influence of changing Holocene insolation on sea surface and thermocline temperatures and compared the results to paleodata [*Liu et al.*, 2003]. Their simulations of 8 ka conditions indicated colder tropical and eastern subtropical annual average SST's and warmer polar, subpolar, and western subtropical regions, in response to an obliquity-related increase in high latitude (and decrease in low latitude) insolation. Precession-related increases in the Northern Hemisphere seasonal cycle (and decreases in the Southern Hemisphere seasonal cycle) during the early Holocene contributed to a latitudinal asymmetry of the high-latitude warming, with much more warming in the north than in the south. Changes in the seasonal cycle also influence the subtropics and midlatitudes more strongly than changes in the annual cycle, in contrast to high and low latitudes. Changes in the seasonal cycle are enhanced on land because of monsoon dynamics, explaining some of the longitudinal variance in records of the Holocene thermal maximum.

[36] A similar compilation of several Northern Hemisphere alkenone records over the Holocene is also consistent with this pattern: Those from the North Atlantic and Mediterranean showed cooling trends, while those from the western tropical Atlantic showed warming trends [*Rimbu et*

al., 2003]. These researchers compared their compilation of paleodata to results from an atmospheric general circulation model, and attributed the overall pattern of Holocene sea surface temperature variability to a weakening of the Arctic Oscillation (AO), considered equivalent to the North Atlantic Oscillation or NAO) because of precession-related insolation changes that warmed the tropics [*Rimbu et al.*, 2003]. The spatial patterns of Holocene climate trends are similar in both these analyses, and consistent with the overall trends of the records shown in Figure 3.

[37] Although the impact of the AO in the tropical Atlantic is weak, and only barely significant in the Southern Hemisphere subtropics, regressions of anomalous SST on the NAO index suggest an antiphased relationship between the subtropical regions at interannual to decadal timescales. Controversy reigns about whether the "Tropical Atlantic Dipole," the opposite meridional trends in interannual SST anomalies apparent in principal component analysis, is significant dynamically [*Chang et al.*, 1997; *Servain et al.*, 2000; *Sutton et al.*, 2000; *Tanimoto and Xie*, 2002; *Andreoli and Kayano*, 2003]. At least one analysis, however, suggests that this interhemispheric mode of coupled ocean-atmosphere variability may actually influence the NAO rather than the other way around [*Ruiz-Barradas et al.*, 2000].

[38] The Hole 1084B record indicates 1°–2°C cooler temperatures in the mid-Holocene between 8.4 and 5.8 ka (see Figure 3c). This shift in temperature is echoed in increases in the relative abundance of *N. pachyderma* (left coiling) (see Figures 2b and 2d), which is consistent with a substantial increase in the intensity of upwelling during this period. The timing of this cool interval is consistent with cool intervals seen in ODP658C, from a similar coastal upwelling area in the Northern Hemisphere subtropics [*deMenocal et al.*, 2000a] (see Figure 3a). This faunal abundance record uses a transfer function for cold and warm season SSTs, suggesting seasonality was much smaller in this location prior to 5.5 ka. Precipitation in the Altiplano of the tropical Andes, as measured from diatom indicators of Lake Titicaca water level and salinity, also dropped substantially between 8.1 and 5.4 ka [*Baker et al.*, 2001]. Both of these studies attribute the timing of mid-Holocene climate shifts to precessional changes in the Earth's orbit and their effect on tropical atmospheric circulation and the maximum latitude of the ITCZ. The $\delta^{18}O$ difference between surface- and thermocline-dwelling planktonic foraminifera in a core off the coast of Brazil in the northwestern tropical Atlantic tracks the depth of the thermocline (or degree of water column stratification), which is forced by the strength of the trade winds [*Arz et al.*, 2001]. This record, although somewhat noisy, has been interpreted to reflect a strengthening of the trade winds at 5.7 ka and 7.2–7.4 ka (see Figure 3d).

[39] The alkenone-derived SST record of *Kim et al.* [2002] does not show any cooling between 8.4 and 5.8 ka, in fact maximum Holocene temperatures occur at 6.4 ka in this record (see Figure 3b). SST estimates from Mg/Ca of *G. ruber* in Cariaco Basin sediments do not show substantial variation in this period either [*Lea et al.*, 2003], nor do Ti and Fe percentages [*Haug et al.*, 2001], although reflectance dips a bit in the mid-Holocene. Perhaps north-south movements of the ITCZ associated with mid-Holocene climate shifts were not quite enough to uniformly affect all Cariaco Basin records, as were those of the Younger Dryas. The *Kim et al.* [2002] record comes from a location which is much farther from the coastal upwelling zones of southwestern Africa than the Hole 1084B record. Perhaps the climate shifts of the mid-Holocene are also not present in the *Kim et al.* [2002] record simply because they were weaker than those of the Younger Dryas.

[40] Alternatively, perhaps the mid-Holocene differences between the alkenone and foraminifera Mg/Ca records can be attributed to changing seasonality of the signals these two proxies represent. *Chapman et al.* [1996] discussed differences seen in late Holocene alkenone and planktonic foraminifera abundance temperature proxies in a subtropical North Atlantic core, concluding that the divergence in the proxies could be explained by slight changes in the season in which the organisms producing alkenones grew. The authors attribute this divergence, which arose about 8 ka and persisted through the rest of the Holocene, to gradual increasing stratification of the upper water column associated with the development of interglacial conditions [*Chapman et al.*, 1996]. So the mechanisms invoked to explain that divergence don't seem applicable to the transient differences between *Kim et al.* [2002] alkenone records and the *G. bulloides* Mg/Ca record presented here. Additionally, the *Kim et al.* [2003] data estimating the strength of the temperature gradient across the Angola-Beguela front (ABF) are consistent with the suggestion that the mid-Holocene discrepancy between the *Kim et al.* [2002] record and the Hole 1084B record may be rooted in different mechanisms of changes in atmospheric circulation, rather than simply being an artifact of the different proxy reconstruction methods. The evidence that the ABF SST gradient was weaker during the Bølling-Alleröd and the early to middle Holocene is consistent with either weaker or more meridional SE trade winds during these times [e.g., *McIntyre and Molfino*, 1996].

5.3. Heinrich Event 1?

[41] The interpretation of the Hole 1084B mid-Holocene upwelling intensification broadens considerably when we look closely at the time period in this record in which Heinrich event 1 (H1) has been documented in other records. According to climate model studies, cooling in the southeastern subtropical Atlantic during H1 would be inconsistent with slower thermohaline circulation and reduced transport of heat across the equator [*Manabe and Stouffer*, 2000; *Vellinga and Wood*, 2002]. The alkenone temperature record of *Kim et al.* [2002] shows consistent warming throughout 15.5–18 ka (see Figure 3b), ruling out the possibility that this location cooled during H1. Our Hole 1084B Mg/Ca temperature record follows a similar overall warming pattern during this period (see Figure 3c), which is consistent with *Kim et al.* [2002]. However, Hole 1084B Mg/Ca SSTs also cool sharply by ~1.5°–1.8°C between 17.7 and 17.2 ka. An even larger and longer-term increase in upwelling intensity is suggested by the increase in *N. pachyderma* (left) abundance between 16.5 and 18.0 ka (see

Figure 2d). Could this possibly be cooling associated with H1? Our age model utilizes the youngest possible calibrated values for many of the radiocarbon dates acquired during this interval (see Figure 2a). However, the unknown possibility of variability in reservoir ages, as discussed above, in addition to the relative uncertainty of the age of H1 itself, mean that we cannot rule out the possibility that the cool interval in Hole 1084B Mg/Ca temperatures between 17.7 and 17.2 ka was associated with H1.

[42] A review by *Hemming* [2004] suggests that *Bond et al.* [1992, 1993] best constrain the age estimate for the beginning of H1 at 14.3–14.6 14°C ka ago. The duration of the event is more difficult to ascertain because of complications due to increased sedimentation rates during the event; best estimates range from 600–1400 years [*Hemming*, 2004]. Assuming a standard reservoir correction of 400 years and taking into account the 2-σ interval of the probability distribution method of converting radiocarbon years to calendar years, the beginning of H1 could lie anywhere between 17.4 and 16.2 ka. Considering the large uncertainty in reservoir corrections for both data sets, it seems possible that the abrupt cool period in Hole 1084B which begins at 17.7 ka may be correlative with H1. If this is so, perhaps the cooler interval between 7.8 and 6.7 ka is associated with the thermocline depth increase seen in the *McIntyre and Molfino* [1996] record during this time. The Hole 1084B cooling at 8.1 ka may have been caused by a mechanism more similar to that of the Younger Dryas. Although only seen in one depth sample, the cooling is replicated in two data points: Perhaps this short-lived temperature change is associated with the "8.2 ky event," in which a sudden release of glacial meltwater into the North Atlantic is hypothesized to have slowed thermohaline circulation [*Barber et al.*, 1999].

[43] Overall, mid-Holocene (8.2–5.8 ka) SSTs at Hole 1084B were cooler than present by 1°–2°C. This interval also corresponds to coolest Holocene SSTs off NW Africa based on faunal assemblage data at Hole 658C [*deMenocal et al.*, 2000b] (Figure 3a). This interval is contemporaneous with the duration of the peak wet phase of the African Humid Period between circa 9 and 6 ka when enhanced Nile River outflow led to the deposition of sapropel S1 in the eastern Mediterranean Sea [*Rossignol-Strick et al.*, 1982]. The cooler SSTs at Hole 658C were associated with faunal changes indicative of enhanced coastal wind-driven upwelling [*deMenocal et al.*, 2000b]. These data suggest the eastern basins of the North and South Atlantic subtropics cooled synchronously between roughly 9–6 ka, coincident with the maximum development of the North African monsoon response to elevated summer-season boreal insolation forcing due to orbital precession.

[44] A key conclusion of the *Liu et al.* [2003] study of coupled ocean-atmosphere response to orbital forcing was that the mid-Holocene orbital configuration was found to enhance the zonal mean tropical trade winds, resulting in upwelling and cooling of the eastern basins of the tropical and subtropical oceans. The effect was particularly pronounced for the southeastern Atlantic where the greatly enhanced North African monsoon invigorated the southeast trade winds and increased upwelling off southwest Africa. The monsoon strengthening stemmed from precession-related increases in the Northern Hemisphere seasonal cycle. The paleoceanographic records from the global tropics compiled by *Liu et al.* [2003] were found to broadly agree with their modeling results. The Hole 1084B and 658C SST records are also consistent with these experiments.

[45] *Kim et al.* [2002, p. 389] note that the "presence of two different SST responses in the Benguela Current system for the H1 and the YD (Younger Dryas) time intervals thus implies that during the YD the so-called bipolar thermohaline circulation effect was weaker than during the H1 period." The possibility of increased Benguela upwelling during H1 and the mid-Holocene suggests an explanation for the differing mechanisms of Heinrich events and the Younger Dryas: Perhaps both are mostly due to perturbations of thermohaline circulation, but with different triggers.

[46] The North Atlantic increase in ice-rafted debris associated with Heinrich events could be forced by precessional linkages to monsoonal circulation, as proposed by *McIntyre and Molfino* [1996], where strengthening the North African monsoon increases the meridionality of SE trade winds. As well as decreasing northward heat transport in the Gulf Stream, this reduces equatorial upwelling (deepening the equatorial thermocline), but increases Southern Hemisphere coastal subtropical upwelling by aligning the predominant wind direction more parallel to the coastline. Therefore SSTs at Hole 1084B cool. SSTs at the *Kim et al.* [2002] site may have remained warm because it is farther from the coastal upwelling cells and changing wind direction doesn't affect upwelling as much as changing wind intensity, or because warmer waters from reduced equatorial upwelling and Gulf Stream heat export are advected to the site by the Equatorial Countercurrent and the Angola Current. In this case the changes in thermohaline circulation would result from orbital changes in insolation, mediated by changes in tropical Atlantic atmospheric circulation.

[47] In the Younger Dryas case, if the initial perturbation stems from sudden releases of fresh water to the North Atlantic, changes in thermohaline circulation are postulated to affect the tropical Atlantic atmospheric circulation. Thermohaline circulation would slow because the decrease in North Atlantic Ocean density from the freshening would reduce North Atlantic Deep Water formation, which would cool the North Atlantic while warming the tropical Atlantic. Estimates of western tropical Atlantic upper ocean temperatures based on stable oxygen isotopes from planktonic foraminifera indicate warming during the Younger Dryas, which is consistent with this scenario [*Arz et al.*, 1999]. This increase in the meridional heat gradient would strengthen the trade winds, increasing both coastal and equatorial Atlantic upwelling.

[48] Complicating the interpretations of all these mechanisms is the inability of the upwelling intensity records to distinguish between changes in trade wind strength and changes in trade wind direction. The attempt to reconstruct the zonal intensity of SW trade winds from the SST gradient across the Angola-Benguela Front starts to address this problem, but the authors still don't always distinguish

clearly between changes in zonality and changes in intensity [*Kim et al.*, 2003]. It is also possible that changes in temperature that are inferred to be due to changes in upwelling intensity may actually be due to changes in preformed temperature of the upwelled water [*Mulitza et al.*, 2002]. The best hints so far that these changes in temperature really do reflect shifts in atmospheric circulation are the simultaneous changes in many proxy records, including thermocline depth in the western part of the basin.

5.4. Holocene Millennial Climate Change

[49] Besides the mid-Holocene shift, there are small variations throughout the Holocene in the Hole 1084B Mg/Ca temperature record. Most in the late Holocene, however, are not significant when compared with the reproducibility of the data set as estimated by the pooled standard deviation, and are only represented by one data point. Sedimentation rates in the middle to late Holocene are also the lowest in the record: Between 8.3 ka and present, time steps between samples ranged from 110 to 150 years. Before 8.3 ka, however, Hole 1084B sedimentation rates were high enough that time steps between samples ranged from 40 to 60 years (Table 1 average time steps column). This period includes four of the five largest Holocene pulses of ice rafting in the North Atlantic, events 5–8 [*Bond et al.*, 2001]: Comparison of the two records does not show any striking correspondence, with the notable exception of the Preboreal oscillation near 11.3 ka (Figures 4c and 4d). Further records with consistently better resolution will be needed to say whether these millennial events, seen elsewhere in the Atlantic [*deMenocal et al.*, 2000a; *Arz et al.*, 2001] and Indian [*Gupta et al.*, 2003] oceans, have a truly global signal.

[50] The Hole 1084 SST record documents the late Holocene "neoglacial" cooling trend which is so evident in many records from the North Atlantic subpolar and subtropical regions [*Keigwin*, 1996; *Bond et al.*, 1997; *deMenocal et al.*, 2000b]. Interestingly, even though the Little Ice Age seems to correspond to one of the smaller North Atlantic ice-rafting pulses (event "zero" in the *Bond et al.* [2001] record), it seems to have a relatively larger expression in the Hole 1084B record. The Mg/Ca temperature of 12.6°C at 0.3 ka is 1.2°–1.6°C cooler than more recent data (see Figure 3c). The pattern of these temperature changes is similar to the pattern in *deMenocal et al.*'s [2000a] faunal abundance-based SST estimates from Hole 1084B in the NE tropical Atlantic (Figure 3a). The thermocline also deepened during these intervals in the *Arz et al.* [2001] record off the coast of Brazil (see Figure 3d). No such temperature changes are seen in the *Kim et al.* [2002] alkenone record (Figure 3b), however, although a lack of radiocarbon dates in sediments younger than 1.9 ka in this record means that the most recent sediments could be missing or disturbed. It is unclear why the Little Ice Age should have such a strong global signature compared to other millennial-scale Holocene events. Perhaps if a persistent millennial climate mechanism operates in the North Atlantic, as suggested by *Bond et al.* [1997, 2001] and *deMenocal et al.* [2000a], its signal only reaches the South Atlantic during the lower latitudinal insolation differences of the late Holocene.

6. Conclusions

[51] Fifteen radiocarbon dates provide a detailed age model for the last 21,000 years in Hole 1084B sediments, although improvements are needed in the estimation of local marine radiocarbon reservoir effects on the age model. Temperatures estimated from the Mg/Ca in core top samples match modern wintertime SST, and faunal abundance and Mg/Ca data are similar. This is consistent with shifts in these proxies largely representing changes in upwelling intensity, although other influences on SST cannot be ruled out. Changes in advection of the coastal current, changes in temperature at the source region for the water being upwelled, and changes in the seasonality of the upwelling are all possible. Comparison with other high-resolution tropical Atlantic paleoclimate records highlights some consistent climate patterns despite these uncertainties.

[52] Taking into consideration the possible effects of differential carbonate dissolution, the Hole 1084B Mg/Ca SST record implies a temperature increase of 2°–3°C between the Younger Dryas and early Holocene, and an increase of 4°–5°C between the LGM and early Holocene. This is consistent with results obtained from the alkenone proxy in a nearby core [*Kim et al.*, 2002], despite unresolved questions about timing offsets between alkenone and foraminiferal radiocarbon ages [*Mollenhauer et al.*, 2003]. In contrast with the nearby alkenone record, however, ODP1084 Mg/Ca temperatures cool during the mid-Holocene. A similar mid-Holocene cool interval is seen in an upwelling zone off the coast of Mauritania in the NE tropical Atlantic [*deMenocal et al.*, 2000b], and the thermocline deepened in the western tropical Atlantic warm pool [*Arz et al.*, 2001]. The different proxies in these distant locations imply basin-wide shifts in atmospheric circulation during the mid-Holocene and Younger Dryas periods, suggesting that much of the temperature changes in the Mg/Ca record are due to variations in the intensity of coastal upwelling.

[53] A brief but significant drop in ODP1084 Mg/Ca temperatures between 17.8 and 17.2 ka could be associated with Heinrich event 1, in which case a cool interval between 7.8 and 6.7 ka in this record could be due to strengthened meridional winds and associated with a Heinrich-like deepening of the eastern tropical Atlantic thermocline. This would be consistent with a tropical origin of Heinrich events [*McIntyre and Molfino*, 1996]. A lack of a cool interval during these times in a nearby alkenone record [*Kim et al.*, 2002] is consistent with this scenario because that site is farther from the coastal upwelling cells and the Benguela current, and more influenced by the Equatorial Countercurrent. While overall strengthening of the trade winds increases equatorial upwelling and contributes to cooling at this site during the Younger Dryas, an increase in the meridionality of the trade winds triggered by insolation changes would decrease equatorial upwelling and warm this site during Heinrich events. A comparison of alkenone

temperatures across the Angola-Benguela front which indicates weakening of at least the zonal component of SE trade winds during the mid-Holocene [*Kim et al.*, 2003] is consistent with the expected differences in atmospheric circulation from these different triggers.

[54] Despite correlation between North Atlantic ice-rafting pulses [*Bond et al.*, 2001] and upwelling intensity in the NE tropical Atlantic, this correlation does not appear to extend to Hole 1084B, a similar coastal upwelling zone in the SE tropical Atlantic, with the exception of the Little Ice Age. Variability on these timescales in the Hole 1084B Mg/Ca temperatures is difficult to distinguish from noise in the record, however. Better spatial and temporal coverage of these kinds of high-resolution paleoclimate records of the glacial-Holocene transition and associated millennial-scale climate changes are necessary in order to determine the mechanisms causing these events.

[55] **Acknowledgments.** We thank John Chiang, Jung-Hyun Kim, Gesine Mollenhauer, Jean Lynch-Stieglitz, Martin Visbeck, and two anonymous reviewers for helpful discussion and insightful comments on earlier drafts. This work would not have been possible without generous assistance from many others: Walter Hale of the ODP core repository in Bremen supplied samples; Martha Bryan helped with picking and sample preparation; Dan Schrag and Ethan Goddard provided initial training on their ICP-OES; and Tom Guilderson performed radiocarbon analyses. ECF was supported by a Graduate Research Environmental Fellowship from the Global Change Education Program, which is administered by the Oak Ridge Institute for Science and Education for the U.S. Department of Energy's Office of Biological and Environmental Research. The LDEO Climate Center and NSF Marine Geology and Geophysics program also provided support. This is Lamont-Doherty Earth Observatory publication number 6693.

References

Alley, R. B., et al. (1993), Abrupt increase in Greenland snow accumulation at the end of the Younger Dryas event, *Nature*, *362*(6420), 527–529.

Andreoli, R. V., and M. T. Kayano (2003), Evolution of the equatorial and dipole modes of the sea-surface temperature in the tropical Atlantic at decadal scale, *Meteorol. Atmos. Phys.*, *83*(3–4), 277–285.

Arz, H. W., J. Patzold, and G. Wefer (1999), The deglacial history of the western tropical Atlantic as inferred from high resolution stable isotope records off northeastern Brazil, *Earth Planet. Sci. Lett.*, *167*(1–2), 105–117.

Arz, H. W., S. Gerhardt, J. Patzold, and U. Rohl (2001), Millennial-scale changes of surface- and deep-water flow in the western tropical Atlantic linked to Northern Hemisphere high-latitude climate during the Holocene, *Geology*, *29*(3), 239–242.

Baker, P. A., G. O. Seltzer, S. C. Fritz, R. B. Dunbar, M. J. Grove, P. M. Tapia, S. L. Cross, H. D. Rowe, and J. P. Broda (2001), The history of South American tropical precipitation for the past 25,000 years, *Science*, *291*(5504), 640–643, doi:10.1126/science.291.5504.640.

Barber, D. C., et al. (1999), Forcing of the cold event of 8,200 years ago by catastrophic drainage of Laurentide lakes, *Nature*, *400*(6742), 344–348, doi:10.1038/22504.

Berger, A., and M. F. Loutre (1997), Intertropical latitudes and precessional and half-precessional cycles, *Science*, *278*(5342), 1476–1478, doi:10.1126/science.278.5342.1476.

Berger, W. H., and G. Wefer (2002), On the reconstruction of upwelling history: Namibia upwelling in context, *Mar. Geol.*, *180*(1–4), 3–28.

Birks, C. J. A., and N. Koc (2002), A high-resolution diatom record of late-Quaternary sea-surface temperatures and oceanographic conditions from the eastern Norwegian Sea, *Boreas*, *31*(4), 323–344, doi:10.1080/030094802320942545.

Blunier, T., et al. (1998), Asynchrony of Antarctic and Greenland climate change during the last glacial period, *Nature*, *394*(6695), 739–743, doi:10.1038/29447.

Boltovskoy, E., D. Boltovskoy, and F. Brandini (2000), Planktonic foraminifera from southwestern Atlantic epipelagic waters: Abundance, distribution and year-to-year variations, *J. Mar. Biol. Assoc. U. K.*, *80*(2), 203–213.

Bond, G., et al. (1992), Evidence for massive discharges of icebergs into the North Atlantic Ocean during the last glacial period, *Nature*, *360*(6401), 245–249.

Bond, G., W. S. Broecker, S. Johnsen, J. McManus, L. Labeyrie, J. Jouzel, and G. Bonani (1993), Correlations between climate records from North Atlantic sediments and Greenland ice, *Nature*, *365*, 143–147.

Bond, G., W. Showers, M. Cheseby, R. Lotti, P. Almasi, P. B. deMenocal, P. Priore, H. M. Cullen, I. Hajdas, and G. Bonani (1997), A pervasive millennial-scale cycle in North Atlantic Holocene and glacial climates, *Science*, *278*, 1257–1266, doi:10.1126/science.278.5341.1257.

Bond, G., B. Kromer, J. Beer, R. Muscheler, M. N. Evans, W. Showers, S. Hoffmann, R. Lotti-Bond, I. Hajdas, and G. Bonani (2001), Persistent solar influence on north Atlantic climate during the Holocene, *Science*, *294*(5549), 2130–2136, doi:10.1126/science.1065680.

Boyle, E. A., and L. D. Keigwin (1985), Comparison of Atlantic and Pacific paleochemical records for the last 215,000 Years—Changes in deep ocean circulation and chemical inventories, *Earth Planet. Sci. Lett.*, *76*(1–2), 135–150.

Boyle, E. A., and L. Keigwin (1987), North-Atlantic thermohaline circulation during the past 20,000 years linked to high-latitude surface-temperature, *Nature*, *330*(6143), 35–40.

Boyle, E. A., and Y. Rosenthal (1996), Chemical hydrography of the South Atlantic during the Last Glacial Maximum: Cd vs. $\delta^{13}C$, *The South Atlantic: Present and Past Circulation*, edited by W. H. Berger, G. Siedler, and D. J. Webb, pp. 423–443, Springer, New York.

Broecker, W. S. (2003), Does the trigger for abrupt climate change reside in the ocean or in the atmosphere?, *Science*, *300*(5625), 1519–1522, doi:10.1126/science.1083797.

Bubnov, G. G., and A. G. Kostianoy (2001), Study of local cells of the Benguela upwelling from satellite data, *Earth Obs. Remote Sens.*, *16*(5), 739–749.

Chang, P., L. Ji, and H. Li (1997), A decadal climate variation in the tropical Atlantic Ocean from thermodynamic air-sea interactions, *Nature*, *385*(6616), 516–518.

Chapman, M. R., N. J. Shackleton, M. Zhao, and G. Eglinton (1996), Faunal and alkenone reconstructions of subtropical North Atlantic surface hydrography and paleotemperature over the last 28 kyr, *Paleoceanography*, *11*(3), 343–357.

Clement, A. C., M. A. Cane, and R. Seager (2001), An orbitally driven tropical source for abrupt climate change, *J. Clim.*, *14*(11), 2369–2375, doi:10.1175/1520-0442(2001)014<2369:AODTSF>2.0.CO;2.

Conkright, M. E., S. Levitus, T. D. O'Brien, T. P. Boyer, J. I. Antonov, and C. Stephens (1998), World Ocean Atlas 1998 [CD-ROM], Natl. Oceanogr. Data Cent., Silver Spring, Md. (Available at http://www.nodc.noaa.gov/OC5/docv2.html)

Conkright, M. E., R. A. Locarnini, H. E. Garcia, T. D. O'Brien, T. P. Boyer, C. Stephens, and J. I. Antonov (2002), World Ocean Atlas 2001: Objective Analyses, Data Statistics, and Figures [CD-ROM], Natl. Oceanogr. Data Cent., Silver Spring, Md. (Available at http://www.nodc.noaa.gov/OC5/WOA01/docwoa01.html)

Dekens, P. S., D. W. Lea, D. K. Pak, and H. J. Spero (2002), Core top calibration of Mg/Ca in tropical foraminifera: Refining paleotemperature estimation, *Geochem. Geophys. Geosyst.*, *3*(4), 1022, doi:10.1029/2001GC000200.

deMenocal, P., J. Ortiz, T. Guilderson, and M. Sarnthein (2000a), Coherent high- and low-latitude climate variability during the Holocene warm period, *Science*, *288*(5474), 2198–2202, doi:10.1126/science.288.5474.2198.

deMenocal, P. B., J. Ortiz, T. Guilderson, J. Adkins, M. Sarnthein, L. Baker, and M. Yarusinsky (2000b), Abrupt onset and termination of the African Humid Period: Rapid climate responses to gradual insolation forcing, *Quat. Sci. Rev.*, *19*(1–5), 347–361, doi:10.1016/S0277-3791(99)00081-5.

Demezhko, D. Y., and V. A. Shchapov (2001), 80,000 years ground surface temperature history inferred from the temperature-depth log measured in the superdeep hole SG-4 (the Urals, Russia), *Global Planet Change*, *29*(3–4), 219–230, doi:10.1016/S0921-8181(01)00091-1.

Duplessy, J. C., E. Ivanova, I. Murdmaa, M. Paterne, and L. Labeyrie (2001), Holocene paleoceanography of the northern Barents Sea and variations of the northward heat transport by the Atlantic Ocean, *Boreas*, *30*(1), 2–16, doi:10.1080/03009480118702.

Elderfield, H., and G. Ganssen (2000), Past temperature and $\delta^{18}O$ of surface ocean waters

inferred from foraminiferal Mg/Ca ratios, *Nature*, *405*(6785), 442–445, doi:10.1038/35013033.

Giraudeau, J. (1993), Planktonic foraminiferal assemblages in surface sediments from the southwest African continental-margin, *Mar. Geol.*, *110*(1–2), 47–62, doi:10.1016/0025-3227(93)90104-4.

Giraudeau, J., and J. Rogers (1994), Phytoplankton biomass and sea-surface temperature estimates from sea-bed distribution of nannofossils and planktonic-foraminifera in the Benguela upwelling system, *Micropaleontology*, *40*(3), 275–285.

Giraudeau, J., G. W. Bailey, and C. Pujol (2000), A high-resolution time-series analyses of particle fluxes in the northern Benguela coastal upwelling system: Carbonate record of changes in biogenic production and particle transfer processes, *Deep Sea Res., Part II*, *47*(9–11), 1999–2028, doi:10.1016/S0967-0645(00)00014-X.

Gordon, A. L., K. T. Bosley, and F. Aikman (1995), Tropical Atlantic water within the Benguela upwelling system at 27°S, *Deep Sea Res., Part I*, *42*(1), 1–12, doi:10.1016/0967-0637(94)00032-N.

Gupta, A. K., D. M. Anderson, and J. T. Overpeck (2003), Abrupt changes in the Asian southwest monsoon during the Holocene and their links to the North Atlantic Ocean, *Nature*, *421*(6921), 354–357, doi:10.1038/nature01340.

Haug, G. H., K. A. Hughen, D. M. Sigman, L. C. Peterson, and U. Rohl (2001), Southward migration of the intertropical convergence zone through the Holocene, *Science*, *293*(5533), 1304–1308, doi:10.1126/science.1059725.

Hemming, S. R. (2004), Heinrich events: Massive late Pleistocene detritus layers of the North Atlantic and their global climate imprint, *Rev. Geophys.*, *42*(1), RG1005, doi:10.1029/2003RG000128.

Hughen, K. A., J. T. Overpeck, S. J. Lehman, M. Kashgarian, J. Southon, L. C. Peterson, R. Alley, and D. M. Sigman (1998), Deglacial changes in ocean circulation from an extended radiocarbon calibration, *Nature*, *391*(6662), 65–68, doi:10.1038/34150.

Hughen, K. A., J. R. Southon, S. J. Lehman, and J. T. Overpeck (2000), Synchronous radiocarbon and climate shifts during the last deglaciation, *Science*, *290*(5498), 1951–1954, doi:10.1126/science.290.5498.1951.

Hughen, K., S. Lehman, J. Southon, J. Overpeck, O. Marchal, C. Herring, and J. Turnbull (2004), ^{14}C activity and global carbon cycle changes over the past 50,000 years, *Science*, *303*(5655), 202–207, doi:10.1126/science.1090300.

Iita, A., A. J. Boyd, and C. H. Bartholomae (2001), A snapshot of the circulation and hydrology of the southern and central shelf regions of the Benguela Current in winter 1999, *S. Afr. J. Sci.*, *97*(5–6), 213–217.

Imbrie, J., and N. G. Kipp (1971), A new micropaleontological method for quantitative paleoclimatology: Application to a late Pleistocene Caribbean core, in *The Late Cenozoic Glacial Ages*, edited by K. K. Turekian, pp. 77–31, Yale Univ. Press, New Haven, Conn.

Kalnay, E., et al. (1996), The NCEP/NCAR 40-year reanalysis project, *Bull. Am. Meteorol. Soc.*, *77*(3), 437–471, doi:10.1175/1520-0477(1996)077<0437:TNYRP>2.0.CO;2.

Keigwin, L. (1996), The Little Ice Age and Medieval Warm Period in the Sargasso Sea, *Science*, *274*(5292), 1503–1508, doi:10.1126/science.274.5292.1503.

Kim, J. H., and R. R. Schneider (2003), Low-latitude control of interhemispheric sea-surface temperature contrast in the tropical Atlantic over the past 21 kyears: The possible role of SE trade winds, *Clim. Dyn.*, *21*(3–4), 337–347, doi:10.1007/s00382-003-0341-5.

Kim, J. H., R. R. Schneider, P. J. Muller, and G. Wefer (2002), Interhemispheric comparison of deglacial sea-surface temperature patterns in Atlantic eastern boundary currents, *Earth Planet. Sci. Lett.*, *194*(3–4), 383–393, doi:10.1016/S0012-821X(01)00545-3.

Kim, J. H., R. R. Schneider, S. Mulitza, and P. J. Muller (2003), Reconstruction of SE trade-wind intensity based on sea-surface temperature gradients in the southeast Atlantic over the last 25 kyr, *Geophys. Res. Lett.*, *30*(22), 2144, doi:10.1029/2003GL017557.

Koutavas, A., J. Lynch-Stieglitz, T. M. Marchitto, and J. P. Sachs (2002), El Niño-like pattern in ice age tropical Pacific sea surface temperature, *Science*, *297*(5579), 226–230, doi:10.1126/science.1072376.

Lea, D. W., T. A. Mashiotta, and H. J. Spero (1999), Controls on magnesium and strontium uptake in planktonic foraminifera determined by live culturing, *Geochim. Cosmochim. Acta*, *63*(16), 2369–2379, doi:10.1016/S0016-7037(99)00197-0.

Lea, D. W., D. K. Pak, L. C. Peterson, and K. A. Hughen (2003), Synchroneity of tropical and high-latitude Atlantic temperatures over the last glacial termination, *Science*, *301*(5638), 1361–1364, doi:10.1126/science.1088470.

Liu, Z., E. Brady, and J. Lynch-Stieglitz (2003), Global ocean response to orbital forcing in the Holocene, *Paleoceanography*, *18*(2), 1041, doi:10.1029/2002PA000819.

Lutjeharms, J. R. E., and J. M. Meeuwis (1987), The extent and variability of southeast Atlantic upwelling, *S. Afr. J. Mar. Sci.*, *5*, 51–62.

Manabe, S., and R. J. Stouffer (1997), Coupled ocean-atmosphere model response to freshwater input: Comparison to Younger Dryas event, *Paleoceanography*, *12*(2), 321–326, (Correction, *Paleoceanography*, *12* (5), 728, 1997.)

Manabe, S., and R. J. Stouffer (2000), Study of abrupt climate change by a coupled ocean-atmosphere model, *Quat. Sci. Rev.*, *19*(1–5), 285–299.

Mashiotta, T. A., D. W. Lea, and H. J. Spero (1999), Glacial-interglacial changes in Subantarctic sea surface temperature and $\delta^{18}O$-water using foraminiferal Mg, *Earth Planet. Sci. Lett.*, *170*(4), 417–432, doi:10.1016/S0012-821X(99)00116-8.

McIntyre, A., and B. Molfino (1996), Forcing of Atlantic equatorial and subpolar millennial cycles by precession, *Science*, *274*(5294), 1867–1870, doi:10.1126/science.274.5294.1867.

Mix, A. C., W. F. Ruddiman, and A. McIntyre (1986), Late Quaternary paleoceanography of the tropical Atlantic. 1: Spatial variability of annual mean sea-surface temperatures, 0–20,000 years B. P., *Paleoceanography*, *1*(1), 43–66.

Mollenhauer, G., T. I. Eglinton, N. Ohkuchi, R. R. Schneider, P. J. Muller, P. M. Grootes, and J. Rullkotter (2003), Asynchronous alkenone and foraminifera records from the Benguela upwelling system, *Geochim. Cosmochim. Acta*, *67*(12), 2157–2171, doi:10.1016/S0016-7037(03)00168-6.

Mulitza, S., A. Paul, C. Schäfer-Neth, S. Rathmann, and G. Wefer (2002), Glacial cooling in the upwelling region off Namibia: Changes in upwelling intensity or preformed temperature?, *Eos Trans. AGU*, *83*(47), Fall Meet. Suppl., Abstract PP21C-0336.

Oberhansli, H., C. Benier, G. Meinecke, H. Schmidt, R. Schneider, and G. Wefer (1992), Planktonic foraminifers as tracers of ocean currents in the eastern South Atlantic, *Paleoceanography*, *7*(5), 607–632.

Ohkouchi, N., T. I. Eglinton, L. D. Keigwin, and J. M. Hayes (2002), Spatial and temporal offsets between proxy records in a sediment drift, *Science*, *298*(5596), 1224–1227, doi:10.1126/science.1075287.

Pahnke, K., R. Zahn, H. Elderfield, and M. Schulz (2003), 340,000-year centennial-scale marine record of Southern Hemisphere climatic oscillation, *Science*, *301*(5635), 948–952, doi:10.1126/science.1084451.

Peterson, L. C., G. H. Haug, K. A. Hughen, and U. Rohl (2000), Rapid changes in the hydrologic cycle of the tropical Atlantic during the last glacial, *Science*, *290*(5498), 1947–1951, doi:10.1126/science.290.5498.1947.

Poole, R., and M. Tomczak (1999), Optimum multiparameter analysis of the water mass structure in the Atlantic Ocean thermocline, *Deep Sea Res. Part I*, *46*(11), 1895–1921, doi:10.1016/S0967-0637(99)00025-4.

Prell, W. L., and W. B. Curry (1981), Faunal and Isotopic indexes of monsoonal upwelling—Western Arabian Sea, *Oceanol. Acta*, *4*(1), 91–98.

Razjigaeva, N. G., A. M. Korotky, T. A. Grebennikova, L. A. Ganzey, L. M. Mokhova, V. B. Bazarova, L. D. Sulerzhitsky, and K. A. Lutaenko (2002), Holocene climatic changes and environmental history of Iturup Island, Kurile Islands, northwestern Pacific, *Holocene*, *12*(4), 469–480, doi:10.1191/0959683602hl549rp.

Rimbu, N., G. Lohmann, J. H. Kim, H. W. Arz, and R. Schneider (2003), Arctic/North Atlantic Oscillation signature in Holocene sea surface temperature trends as obtained from alkenone data, *Geophys. Res. Lett.*, *30*(6), 1280, doi:10.1029/2002GL016570.

Rosenthal, Y., and G. P. Lohmann (2002), Accurate estimation of sea surface temperatures using dissolution-corrected calibrations for Mg/Ca paleothermometry, *Paleoceanography*, *17*(3), 1044, doi:10.1029/2001PA000749.

Rossignol-Strick, M., W. Nesteroff, P. Olive, and C. Vergnaudgrazzini (1982), After the deluge—Mediterranean stagnation and sapropel formation, *Nature*, *295*(5845), 105–110, doi:10.1038/32631.

Ruhlemann, C., S. Mulitza, P. J. Muller, G. Wefer, and R. Zahn (1999), Warming of the tropical Atlantic Ocean and slowdown of thermohaline circulation during the last deglaciation, *Nature*, *402*(6761), 511–514, doi:10.1038/990069.

Ruiz-Barradas, A., J. A. Carton, and S. Nigam (2000), Structure of interannual-to-decadal climate variability in the tropical Atlantic sector, *J. Clim.*, *13*(18), 3285–3297, doi:10.1175/1520-0442(2000)013<3285:SOITDC>2.0.CO;2.

Schrag, D. P. (1999), Rapid analysis of high-precision Sr/Ca ratios in corals and other marine carbonates, *Paleoceanography*, *14*(2), 97–102.

Servain, J., I. Wainer, H. L. Ayina, and H. Roquet (2000), The relationship between the simulated climatic variability modes of the tropical Atlantic, *Int. J. Climatol.*, *20*(9), 939–953, doi:10.1002/1097-0088

(200007)20:9<939::AID-JOC511>3.0.CO;2-V.

Southon, J., M. Kashgarian, M. Fontugne, B. Metivier, and W. W. S. Yim (2002), Marine reservoir corrections for the Indian Ocean and southeast Asia, *Radiocarbon*, *44*(1), 167–180.

Staubwasser, M., F. Sirocko, P. M. Grootes, and H. Erlenkeuser (2002), South Asian monsoon climate change and radiocarbon in the Arabian Sea during early and middle Holocene, *Paleoceanography*, *17*(4), 1063, doi:10.1029/2000PA000608.

Steig, E. J., E. J. Brook, J. W. C. White, C. M. Sucher, M. L. Bender, S. J. Lehman, D. L. Morse, E. D. Waddington, and G. D. Clow (1998), Synchronous climate changes in Antarctica and the North Atlantic, *Science*, *282*(5386), 92–95, doi:10.1126/science.282.5386.92.

Stotter, J., M. Wastl, C. Caseldine, and T. Haberle (1999), Holocene palaeoclimatic reconstruction in northern Iceland: Approaches and results, *Quat. Sci. Rev.*, *18*(3), 457–474, doi:10.1016/S0277-3791(98)00029-8.

Stuiver, M., and P. M. Grootes (2000), GISP2 oxygen isotope ratios, *Quat. Res.*, *53*(3), 277–283, doi:10.1006/qres.2000.2127.

Stuiver, M., and P. J. Reimer (1993), Extended C-14 data-base and revised calib 3.0 C-14 age calibration program, *Radiocarbon*, *35*(1), 215–230.

Stute, M., and A. S. Talma (1998), Glacial temperatures and moisture transport regimes reconstructed from noble gases and $\delta^{18}O$, Stampriet Aquifer, Namibia, in *Isotope Techniques in the Study of Environmental Change: Proceedings of the International Symposium on Isotope Techniques in the Study of Past and Current Environmental Changes in the Hydrosphere and the Atmosphere*, pp. 307–318, Int. At. Energy Agency, Vienna.

Stute, M., M. Forster, H. Frischkorn, A. Serejo, J. F. Clark, P. Schlosser, W. S. Broecker, and G. Bonani (1995), Cooling of tropical Brazil (5°C) during the last glacial maximum, *Science*, *269*(5222), 379–383.

Sutton, R. T., S. P. Jewson, and D. P. Rowell (2000), The elements of climate variability in the tropical Atlantic region, *J. Clim.*, *13*(18), 3261–3284, doi:10.1175/1520-0442(2000)013<3261:TEOCVI>2.0.CO;2.

Tanimoto, Y., and S. P. Xie (2002), Inter-hemispheric decadal variations in SST, surface wind, heat flux and cloud cover over the Atlantic Ocean, *J. Meteorol. Soc. Jpn.*, *80*(5), 1199–1219.

Vellinga, M., and R. A. Wood (2002), Global climatic impacts of a collapse of the Atlantic thermohaline circulation, *Clim. Change*, *54*(3), 251–267, doi:10.1023/A:1016168827653.

Zhao, M. X., G. Eglinton, S. K. Haslett, R. W. Jordan, M. Sarnthein, and Z. H. Zhang (2000), Marine and terrestrial biomarker records for the last 35,000 years at ODP site 658C off NW Africa, *Org. Geochem.*, *31*(9), 919–930, doi:10.1016/S0146-6380(00)00027-9.

P. B. deMenocal, Lamont-Doherty Earth Observatory of Columbia University, Palisades, NY 10964-8000, USA.

E. C. Farmer, Geology Department, Hofstra University, 145 Gittleson, Hempstead, NY 11549-1140, USA. (christa@ldeo.columbia.edu)

T. M. Marchitto, Department of Geological Sciences and Institute of Arctic and Alpine Research, University of Colorado, Boulder, CO 80309-0450, USA.